

Characterization of Polycyclic Aromatic Hydrocarbon Particulate and Gaseous Emissions from Polystyrene Combustion

SUSAN K. DURLAK AND PRATIM BISWAS*

Aerosol and Air Quality Research Laboratory, Department of Civil and Environmental Engineering, University of Cincinnati, Cincinnati, Ohio 45221-0071

JICHUN SHI AND MARY JO BERNHARD

Environmental Science Department, The Procter & Gamble Company, 5299 Spring Grove Avenue, Cincinnati, Ohio 45217-1087

The partitioning of polycyclic aromatic hydrocarbons (PAHs) between the particulate and gaseous phases resulting from the combustion of polystyrene was studied. A vertical tubular flow furnace was used to incinerate polystyrene spheres (100–300 μm) at different combustion temperatures (800–1200 $^{\circ}\text{C}$) to determine the effect of temperature and polystyrene feed size on the particulate and gaseous emissions and their chemical composition. The furnace reactor exhaust was sampled using real-time instruments (differential mobility particle sizer and/or optical particle counter) to determine the particle size distribution. For chemical composition analyses, the particles were either collected on Teflon filters or split into eight size fractions using a cascade impactor with filter media substrates, while the gaseous products were collected on XAD-2 adsorbent. Gas chromatography/mass spectroscopy (GC/MS) was used to identify and quantify the specific PAH species, their partitioning between the gas and particulate phases, and their distribution as a function of emission particle size. The total mass and number of PAH species in both the particulate and gas phases were found to decrease with increasing incineration temperature and decreasing polystyrene feed size, while the mean diameter of the particles increases with increasing incineration temperature and decreasing feed size. In addition, the PAH species in the particulate phase were found to be concentrated in the smaller aerosol sizes. The experimental results have been analyzed to elucidate the formation mechanisms of PAHs and particles during polystyrene combustion. The implications of these results are also discussed with respect to the control of PAH emissions from municipal waste-to-energy incineration systems.

Introduction

Incineration is currently the focus of much research and regulatory effort, due in part to the potentially toxic trace organic compounds generated as products of incomplete combustion. While emissions of heavy metals such as

cadmium, lead, and mercury are also of significant concern in municipal solid waste (MSW) incineration (1, 2), trace organic products such as polycyclic aromatic hydrocarbons (PAHs) from incomplete combustion are of special concern due to the potential carcinogenicity for some of these compounds. A major source of PAHs from MSW incinerators is high-volume plastics (3–8), which are primarily comprised of polyethylene (65 wt %), polystyrene (22%), polypropylene (9%), and PVC (4%) (3). Previous incineration studies have indicated that combustion of polystyrene leads to a significantly larger amount of PAHs than the other plastics, probably due to its aromatic structure (4–8). A better understanding of the chemical and physical processes that are responsible for PAH emissions from polystyrene combustion will lead to better methods for postcombustion control and, potentially, methods to reduce the formation of these compounds in combustion systems.

The combustion of polystyrene is a complex and not thoroughly understood process. This is especially true of the PAH and soot particle formation mechanisms. When a polymer is combusted, there is generally a two-stage pyrolysis/combustion process. First the polymer is heated, releasing low molecular weight gaseous pyrolysis products followed by higher molecular weight gaseous products. This forms a gas cloud of pyrolysis products around the polystyrene sphere. Next, oxygen diffuses into the pyrolysis product cloud, and a diffusion flame is established (9). In the diffusion flame, soot (fine particulate matter) is formed consisting of agglomerates of particle chains of 10^5 – 10^6 carbon atoms. It has been reported that polystyrene produces a significant amount of fine particles (7, 8). Elomaa and Saharinen (5) have reported that as much as 30–50% of the original mass remains as particulate matter. While the exact formation mechanism of soot in polystyrene combustion is not well understood, several studies have examined the development of soot monomers and aggregates in hydrocarbon flames (10, 11). The development of soot in the flame has been linked to PAH formation and destruction in the flame, with PAH compounds forming early in the flame, via condensation reactions with acetylene (10) or reactive coagulation of smaller PAHs (11).

When the PAHs have been built up to molecules with an approximate molecular weight of 1000, or 100 carbon atoms, soot inception occurs (10). Once soot nuclei are formed, condensation reactions continue to occur at the nuclei surface, resulting in growth to monomers between 0.01 and 0.05 μm (12). Once the soot reaches the monomer size, further growth is by Brownian coagulation.

Previous combustion studies on polystyrene (4, 5, 7, 8) have examined primarily the range of organic compounds, including PAHs, that are formed at various combustion temperatures. Panagiotou and Levendis (7) studied the combustion of large (300 μm) and small (60 μm) polystyrene spheres at 1000 $^{\circ}\text{C}$ using high-speed cinematography, and they found that the small polystyrene spheres were consumed much more quickly (6–7 ms) than the larger ones (120–160 ms). Wheatley et al. (4) examined the PAH emissions resulting from combustion of several plastics and found significant variation with temperature in the range of 750–1150 $^{\circ}\text{C}$. Although Wheatley et al. (4) did not differentiate between the PAHs collected in the particulate and gas phases, other studies (5, 8) have attempted to study partitioning, but variations in the collection techniques introduced considerable uncertainties in the data. Hawley-Fedder et al. (8) differentiated between the PAHs in the particulate and gas

* To whom correspondence should be addressed. Telephone: (513)556-3697; fax: (513)556-2599; e-mail: pratim.biswas@uc.edu.

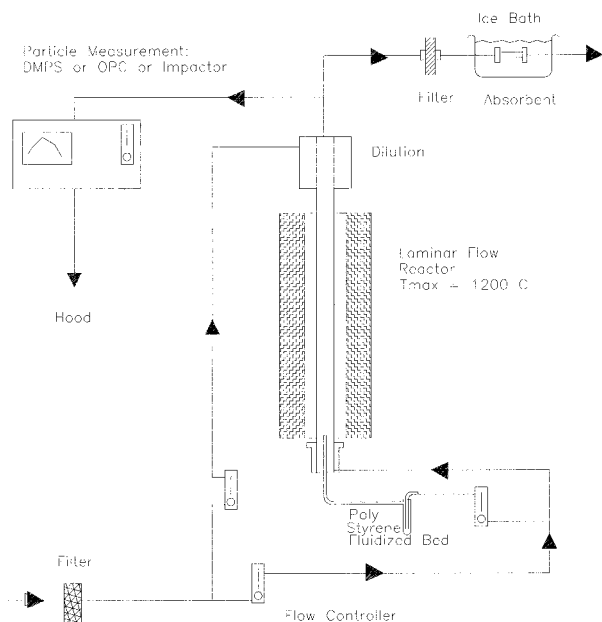


FIGURE 1. Schematic diagram of experimental setup.

phases at 800–950 °C, finding that most of the PAHs (88%) were associated with the soot at 800 °C. As the combustion temperature was increased, however, an increasing fraction of PAHs was found in the gas phase. Despite the high variability in these previous studies, a clear trend of decreasing total PAH yield (in both mass and number of species) with increasing combustion temperature has been reported in the literature. The majority of the PAHs detected have been in the particulate phase.

To the best of our knowledge, no studies have reported the size distributions of the particles formed during polystyrene combustion or determined the PAH chemical composition as a function of particle size. The distribution of the PAHs in different size ranges is an important parameter, as the deposition of particles in the respiratory tract and lung is size dependent. In this study, the trace PAHs in the particulate and gaseous emissions from polystyrene combustion were investigated. Combustion parameters such as furnace temperature and the size of polystyrene feed spheres were varied to determine the effect on resultant particle size, composition as a function of size, and overall partitioning between the gaseous and particulate phases.

Experimental Procedures

The polystyrene combustion experiments were conducted using a vertical, laminar flow, tubular furnace with a maximum temperature of 1200 °C (Figure 1). Dry, particle-free air was mixed with small polystyrene spheres and fed through the furnace reactor. An average of about 130% (by mass) excess air was used for the combustion. The gas residence time in the furnace was approximately 0.5 s. Most MSW incinerators have gas residence times of about 2 s; however, the residence time in this study was long enough to ensure the complete combustion of the polystyrene spheres (combustion time of ~6 to 120 ms) (7). The aerosol dynamics and chemistry were “frozen” at the exit of the reactor by adding dilution air (2:1) at approximately 20 cm downstream of the furnace, resulting in diluted exhaust temperatures approximately half of the initial exhaust temperature, similar to other studies (13, 14). At the sampling location, the diluted exhaust had cooled to less than 90 °C.

The polystyrene sample was purchased as pellet stock polymer (Aldrich, Inc.), frozen with liquid nitrogen, and crushed using a grinder. The polystyrene powder was sieved

into particle size ranges of 250–300 and 104–175 μm . Experiments were performed with these two size ranges of polystyrene feed. The feed rate, on a mass basis, and airflow rate were equivalent in both experiments, maintaining the same fuel-to-air ratio. A microscope photograph of the sieved particles is shown in Figure 2A, and a transmission electron microscope (TEM) picture of the soot agglomerates collected from the furnace exhaust is shown in Figure 2B.

The chemical analysis procedure used in this work is similar to that used by Wheatley et al. (4). A 47- μm Teflon filter (Gelman) was used to capture the particles, and XAD-2 adsorbent (housed in a Teflon tube approximately 10 cm \times 1 cm diameter and cooled with an ice bath) was used to adsorb the gaseous combustion products downstream of the Teflon filter. While there could be considerable uncertainty in accurately assigning the PAH yield to the gas and particulate phases, due to sampling artifacts, studies (15, 16) indicate that using a Teflon filter can minimize the absorption of gaseous compounds onto the filter. Gas-particle partitioning results should be considered a rough estimate, but uncertainty in the partitioning does not affect the accuracy of the total PAH yield, which is the sum of the two phases.

Both the Teflon filters and XAD-2 adsorbent were spiked with two internal standards phenanthrene- d_{10} and benzo[*a*]pyrene- d_{12} ; extracted for 17 h in a Soxhlet apparatus with methylene chloride; concentrated in a rotary evaporator to 1 mL; and stored in sealed, refrigerated vials for analysis. The Soxhlet extracts were analyzed using an HP5890 gas chromatograph with an HP5971 mass spectroscopy detector (using electron ionization). The GC column was a DB-5 MS column with 0.25 mm i.d. \times 30 m length and 0.25 μm film thickness (J&W Scientific). The initial column temperature was set at 50 °C with a heating rate of 15 °C/min and a final column temperature of 300 °C. The mass selective detector was operated in the electron impact mode. The trace combustion products were identified by matching with a mass spectra library (17) and comparison with known retention indices of PAHs from the literature (18, 19). The quantification of the individual combustion products was done by comparison with the two perdeuterated PAH internal standards. As in previous studies (8, 20), a linear interpolation between the two internal deuterated standards was used to estimate the relative response of the identified PAHs. Ideally every compound should be identified and quantified individually using a known standard of that compound; however, this is impractical due to the large number of PAH species observed in polystyrene combustion systems.

The particle size distribution in the furnace exhaust was measured by three complementary instruments, due in part to the large particle size range (from submicrometer to 20 μm and above): an optical particle counter (OPC) for 0.1–3.0 μm , a differential mobility particle sizer (DMPS, TSI) in combination with a condensation nuclei counter (CNC, TSI) for 0.01–1.0 μm , and an eight-stage cascade impactor (Mark 3, Andersen) covering sizes from ~0.28 to >20 μm . The cascade impactor was primarily used to collect particles in various size ranges for chemical analyses.

Results and Discussion

A baseline case with 250–300 μm polystyrene feed spheres combusted at 900 °C was chosen to investigate the PAH partitioning between the gas and particulate phases as well as the PAH distribution as a function of the exhaust particle size. The 900 °C furnace temperature is close to the nominal operating temperature of many state-of-the-art municipal solid waste incinerators (2, 3). Experiments were also conducted to investigate the partitioning and particle size distribution as a function of furnace temperature (800–1200 °C) and the impact of the polystyrene feed sphere size.

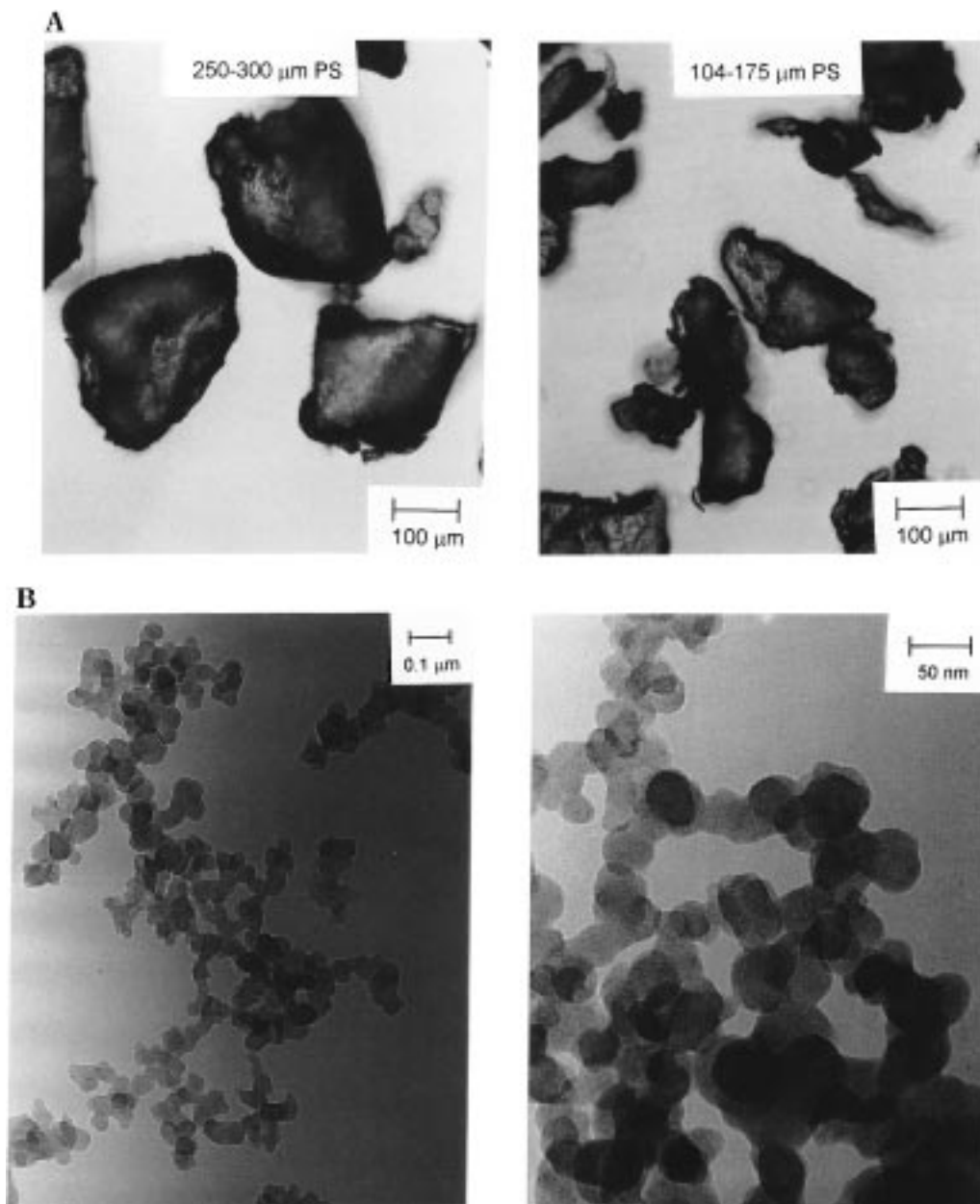


FIGURE 2. (A) Photograph of the polystyrene feed spheres, with size cuts 104–175 and 250–300 μm . (B) Transmission electron microscope (TEM) image of the soot particles collected downstream of the combustor at two magnifications.

Baseline Experiment ($T = 900\text{ }^{\circ}\text{C}$). In the baseline case, about 87% (by total ion abundance) of the eluted compounds from the Teflon filter extract and 75% of the gaseous compounds were identified. The mass yields at $900\text{ }^{\circ}\text{C}$ of individual PAH compounds are summarized in Table 1, Section A, for the filter extract and in Table 1, Section B, for the XAD-2 sorbent extract, respectively.

The most abundant PAH species in the particulate phase were benzo[*j*]fluoranthene, 2,7-dimethylpyrene, pyrene, and dihydronaphthacene, followed by several other, generally higher molecular weight, PAHs. Some of these compounds were observed by Hawley-Fedder et al. (8) in the particulate phase at $900\text{ }^{\circ}\text{C}$ and by Wheatley et al. (4) in both particulate and gas phases at $950\text{ }^{\circ}\text{C}$ (see Table 1). Several other species that were identified in the present filter extract were not found by Hawley-Fedder et al. (8) or by Wheatley et al. (4). The total number of PAH species identified in this work at $900\text{ }^{\circ}\text{C}$ is 36, which is smaller than the 41 species found by Hawley-Fedder et al. (8) but much larger than the eight species

found by Wheatley et al. (4) under similar experimental conditions.

The most abundant PAH species in the gaseous phase were biphenyl, naphthalene, acenaphthylene, and styrene (see Table 1). Again, there were several compounds that were found in the present work but not by Hawley-Fedder et al. (8) or Wheatley et al. (4). As shown in Table 1, the partitioning between the gas and particulate phases was about 65% and 35%, respectively at $900\text{ }^{\circ}\text{C}$. Though previous researchers have not reported a detailed distribution of PAH or their yield, Hawley-Fedder et al. (8) reported a partitioning of total PAH mass (26% gas and 74% particulate matter) that was very different from that reported here at the same combustion temperature. This difference may be due to the variation in the PAH collection methods used in the two experimental systems. Hawley-Fedder et al. (8) used glass wool to trap particles (vs Teflon filters used in this study) and cold traps to trap gas phase PAHs (vs XAD-2 absorbent used here). The large amount of surface area in the glass wool

TABLE 1. PAH Yields under Baseline Conditions (900 °C)^a

PAH species	retention index (Lee Index)	PAH yield (mg/g of PS)	% of total	Hawley-Fedder (70) (900 °C)	Wheatley et al. (6) (950 °C)
Section A: In the Particulate Phase					
naphthalene	200.0	0.105	0.84	x	x
isoquinoline	212.1	0.059	0.47		
biphenyl	231.1	0.066	0.53	x	x
acenaphthylene	245.4	0.036	0.29	x	
4-methyl-9H-fluorene	256.3	0.081	0.64		
9H-fluorene	268.2	0.243	1.94	x	
4-ethenyl-1,1'-biphenyl	270.5	0.105	0.84		
4,4'-dimethyl-biphenyl	274.5	0.120	0.96		
xanthene	279.1	0.134	1.07		
9,10-dihydroanthracene	285.6	0.119	0.95	x	
9,10-dihydrophenanthrene	286.8	0.500	3.99	x	
dibenzothiophene	295.6	0.156	1.25		x
anthracene	301.7	0.650	5.19		x
1-phenylnaphthalene	309.2	0.436	3.48	x	
3-methylphenanthrene	319.4	0.428	3.42	x	x
4,5,9,10-tetrahydropyrene	325.7	0.828	6.61	x	
4,5-dihydropyrene	327.1	0.092	0.73		
2-phenyl-naphthalene	333.9	0.122	0.97	x	
1,4-dihydro-1,4-ethenoanthracene	335.8	0.130	1.04		
2,7-dimethylphenanthrene	339.1	1.114	8.90		
1,2,3,6,7,8-hexahydropyrene	342.3	0.639	5.10		
fluoranthene	344.8	0.185	1.48	x	
pyrene	346.6	0.980	7.82	x	
m-terphenyl	352.6	0.088	0.70	x	
p-terphenyl	357.6	0.374	2.99		
benzo[a]fluorene	359.8	0.270	2.16	x	x
4,5,6-trihydrobenz[de]anthracene	363.5	0.283	2.26		
dihydronaphthacene	380.4	0.978	7.81	x	
2,7-dimethylpyrene	387.0	0.906	7.24		
1,1'-binaphthyl	390.0	0.294	2.35		
1,2'-binaphthyl	406.8	0.395	3.15	x	
2,2'-binaphthyl	412.0	0.316	2.52	x	
benzo[j]fluoranthene	432.9	1.289	10.29		x
total PAH yield (mg/g of PS)		12.52			
% of PAHs in particulate		35.1			
Section B: In the Gaseous Phase					
styrene	135.5	2.078	8.96		
3,5-diphenyl-1,2,4-trioxolane	151.5	2.019	8.71		
indane	169.1	1.262	5.44		
1-ethynyl-4-methylbenzene	169.8	1.401	6.04		
1-phenylethanone	173.9	0.843	3.64		
naphthalene	200.0	3.955	17.06	x	x
quinoline	206.0	0.482	2.08		
biphenyl	235.6	4.249	18.33	x	x
acenaphthylene	249.0	2.136	9.21	x	
4-methyl-9H-fluorene	257.6	0.353	1.52		
1,1'-(1,2-dibromo-1,2-ethanediy)bisbenzene	259.4	0.610	2.63		
4-ethenyl-1,1'-biphenyl	270.6	1.642	7.08		
9-methylfluorene	272.9	0.653	2.81	x	x
9,10-dihydrophenanthrene	287.0	0.289	1.25		
dihydronaphthacene	381.2	1.212	5.23		
total PAH yield (mg/g of PS)		23.18			
% of PAH's in gas phase		64.9%			

^a x indicates detected but not quantified in the literature studies.

was likely to absorb gas phase PAHs and wrongly attribute them to the particulate phase. The setup used in this experiment is more likely to correctly attribute PAHs to the two phases.

In addition to chemical analyses, the aerosol size distribution was measured. The exhaust particle size distribution at 900 °C is shown in Figure 3, which indicates that most of the particles are smaller than 1 μm, with the peak at 0.3–0.4 μm. In addition, there is a general consistency in the measurements of the three instruments over the particle size range measured. Although some discrepancy does exist between the actual number of particles determined on the

basis of the instruments, this is most likely due to assumptions inherent in each method.

The chemical composition as a function of particle size has been investigated using a cascade impactor separating the particles into a total of eight size fractions. The results of the chemical analyses are summarized in Table 2. On average, about 81% (by total ion abundance) of the observed total ion chromatogram peaks have been identified. Several species that were identified in the cascade impactor samples were not found in the “total particulate matter” Teflon filter sample and vice versa. In general, there were more, lower molecular weight PAHs identified in the Teflon filter extract,

TABLE 2. Particulate Size Distribution of the PAHs under Baseline Conditions (900 °C)

PAH species	retention index (Lee Index)	total impactor PAH yield (mg/g)	mean impactor bin size (μm)							
			14.4	6.1	2.5	1.24	0.66	0.36	0.14	
acenaphthylene	245.4	0.05								x
2,3,6-trimethylnaphthalene	265.3	0.04		x						
9H-fluorene	268.2	0.05						x		
4-ethenyl-1,1'-biphenyl	270.5	0.09							x	x
4,4'-dimethyl-biphenyl	274.5	0.02						x		
4,4a,9,10-tetrahydro-4a-methyl-2(3H)-phenanthrene	288.3	0.69	x	x	x	x			x	x
1,2,3,4,5,6,7,8-octahydrophenanthrene	292.3	0.03							x	
dibenzothiophene	295.6	0.09						x	x	
anthracene	301.7	0.08						x		
acridine	303.3	0.19						x	x	x
benzo[f]quinoline	307.3	0.12						x		x
phenanthridine	308.1	0.04							x	
1-phenylnaphthalene	309.2	0.17						x	x	x
1,2,3,10b-tetrahydrofluoranthene	314.6	0.16						x	x	x
3-methylphenanthrene	319.4	0.11						x	x	
o-terphenyl	321.7	0.19	x					x	x	x
4,5,9,10-tetrahydropyrene	325.7	0.32				x		x	x	x
thianthrene	327.9	0.26						x	x	x
2-phenylnaphthalene	333.9	0.03						x		
2,7-dimethylphenanthrene	339.1	0.72		x	x	x	x	x	x	x
1,2,3,6,7,8-texahydropyrene	342.3	0.26				x		x	x	x
fluoranthene	344.8	0.02						x		
pyrene	346.6	1.67	x	x		x		x	x	x
9,10-dimethylanthracene	349.1	0.38	x	x						
p-terphenyl	357.6	0.03						x		
benzo[a]fluorene	359.8	0.13		x				x		
4,5,6-trihydrobenz[de]anthracene	363.5	0.02						x		
5,12-dihydronaphthacene	380.4	3.73	x	x	x	x	x	x	x	x
2,7-dimethylpyrene	387.0	0.35						x	x	x
benzo[c]phenanthrene	394.3	0.44	x	x				x	x	x
cyclopenta[cd]pyrene	395.2	0.03						x		
benzo[a]carbazole	403.5	0.21						x	x	x
naphthacene	407.3	0.45	x					x	x	x
benzo[j]fluoranthene	432.9	0.13						x		
benzo[k]fluoranthene	437.8	0.04						x		
perylene	452.0	0.12	x							
total PAH yield (mg/g of PS)		11.7	2.1	1.2	0.6	0.7	2.3	1.7	3.2	

^a X indicates detected in this impactor size range.

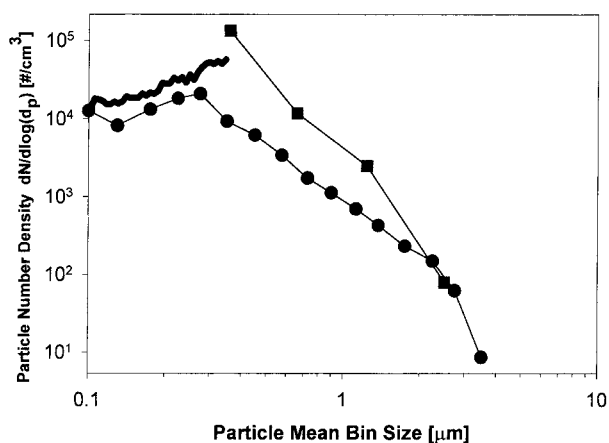


FIGURE 3. Size distribution of the particulates formed in the polystyrene combustion exhaust under baseline conditions (900 °C): (●) Optical particle counter (OPC). (■) Cascade impactor. (Solid line) Differential mobility particle sizer (DMPS).

while more higher molecular weight PAHs were identified in the cascade impactor sample extract. This may be due to the Teflon filter trapping some of the lower molecular weight compounds as the gas flows through the filter. In the cascade impactor, the compounds deposit on the filters by impaction, and the lighter compounds can flow around, not through, the filter material.

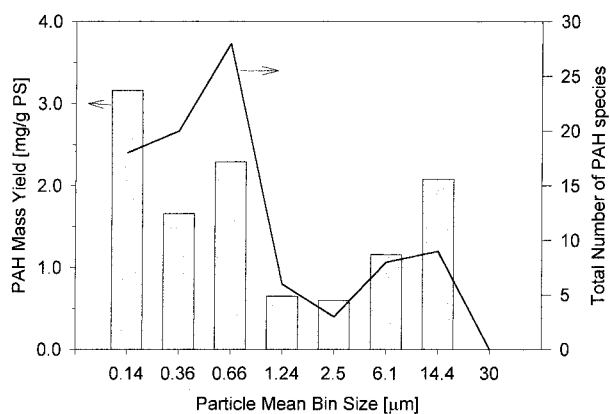


FIGURE 4. Particulate size distribution of the total PAH yield and the number of PAH species under baseline condition (900 °C).

The total mass of the aerosol-associated PAH species was found to vary significantly with the size of the particles. The variation of the number of PAH species and total PAH mass as a function of particle size is shown in Figure 4. There is a bimodal distribution in both the total PAH mass yield and the number of species as a function of particle size, with the minimum between 1 and 2 μm . In addition, there is also significant difference in the molecular weights of the PAH species on the particles above and below 1 μm . As shown in Table 2, the PAHs associated with particles larger than

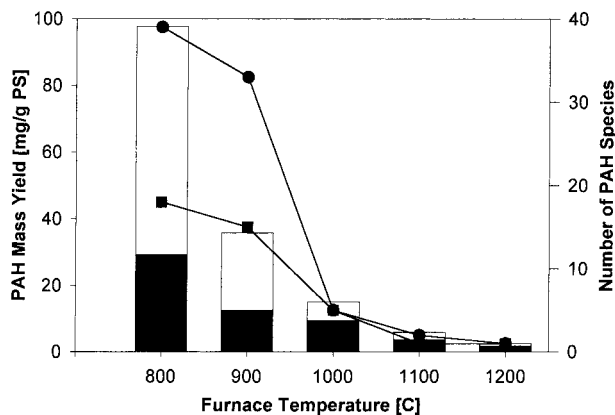


FIGURE 5. Temperature dependence of the PAH yield and the number of PAH species in the gas and particulate phases. (■) PAH yield in the particulate phase. (□) PAH yield in the gas phase. (●) Number of PAH species on the particulates. (■) Number of PAH species in gas phase.

1 μm are primarily those with retention indices larger than fluoranthene (RI = 344.8), while the smaller particles contain PAHs with a wide range of retention indices and presumably molecular weights as well. The total mass of the particles does not have the bimodal distribution observed in the PAH yields; the number size distribution of the particles has a log-normal size distribution, as is normally associated with combustion aerosol, with a mass mean diameter around 1.24 μm . The number mean diameter (Figures 3 and 6) is less than 1.0 μm . The relatively large amount of PAHs associated with the smaller particles (less than 1.0 μm) provides the need for control of fine particulate emissions from incinerators.

Variation with Combustion Temperature. The impact of furnace temperature on polystyrene combustion was investigated at 800, 900, 1000, 1100, and 1200 $^{\circ}\text{C}$. The PAH yields in the gas and particulate phases, as well as the number of PAH species in each phase, are shown in Figure 5. There was an exponential decrease in the total number of PAH species and total mass yields when the combustion temperature was increased from 800 to 1200 $^{\circ}\text{C}$, with virtually no PAHs observed at 1200 $^{\circ}\text{C}$. At lower temperatures, the percentage of PAH mass in the gas phase was substantially higher than in the particulate phase (70% vs 30%), but at the higher temperatures, the reverse was true: at 1100 $^{\circ}\text{C}$, about 70% of the PAH mass is bound with the particles, while 30% was in the gas phase. The size distribution of the particles also varies significantly with the furnace temperature and is shown in Figure 6 for 900 and 1200 $^{\circ}\text{C}$. There is a significant shift to larger particles as the furnace temperature increases. At 900 $^{\circ}\text{C}$, the average particle size is about 0.3 μm , but at 1200 $^{\circ}\text{C}$ it increases to about 1 μm . This increase in particle size may be due to faster combustion at the higher temperatures, allowing more time for the nucleated particles to grow by coagulation and/or condensation into larger sizes in the furnace (as residence time was kept constant).

Variation with Polystyrene Feed Size. To determine the impact of polystyrene feed sphere size, a smaller feed sphere size cut (104–175 μm) was combusted at a furnace temperature of 900 $^{\circ}\text{C}$. The PAH mass yield with the smaller feed spheres is about seven times smaller than with the larger ones (250–300 μm). The yield for the smaller feed spheres is about the same as the larger ones at a much higher furnace temperature (1200 $^{\circ}\text{C}$). In addition, the PAH partitioning is about the same for the smaller feed spheres at 900 $^{\circ}\text{C}$ as for the larger ones at 1200 $^{\circ}\text{C}$. These observations suggest that smaller polystyrene feed spheres lead to more complete combustion at the same furnace temperature. This conclu-

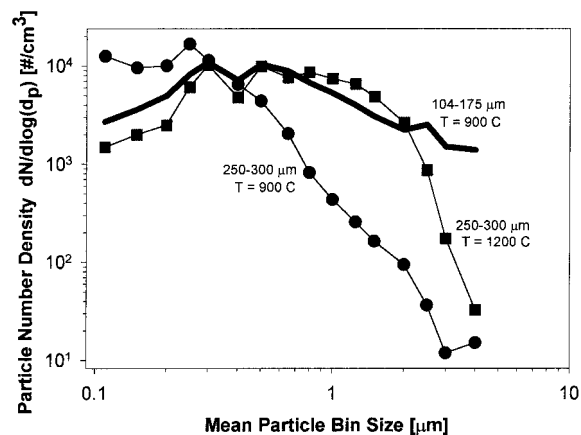


FIGURE 6. Size distribution of particles in the exhaust as measured by the optical particle counter (OPC) for two different feed particle sizes and at two furnace temperatures.

sion is consistent with previous studies by Panagiotou and Levendis (7), who reported that the smaller polystyrene spheres burn faster in the furnace and thus have longer time to burn more completely, although the overall combustor residence time is approximately the same with both feed sphere sizes.

The more complete combustion of smaller polystyrene feed spheres is reinforced by the resultant exhaust particle size distribution. As shown in Figure 6, the exhaust particle size distribution for the smaller feed spheres at 900 $^{\circ}\text{C}$ is similar to that for the larger feed spheres at 1200 $^{\circ}\text{C}$. The significant impact of the feed sphere size suggests that the total PAH mass yield is highly correlated with combustion condition even at the same furnace temperature. Therefore, care must be taken in extrapolating the PAH mass yield data from the laboratory experiments to full-scale municipal solid waste incinerators.

Mechanistic Implications. The experimental results summarized above can be used to make some observations about the mechanisms of incineration of polystyrene under municipal solid waste incinerator conditions. First, the decrease in the PAH yield with increasing combustion temperature and smaller feed sphere size (as shown in Figures 5 and 6) indicate that these conditions lead to both faster pyrolysis and gas-phase combustion reaction rates in the diffusion flame zone and thus more complete combustion. Second, there is a shift to heavier PAHs and larger particles with more complete combustion, either at higher furnace temperature or with smaller feed spheres. These observations are consistent with the mechanism that includes the formation of larger PAH molecules through the agglomeration of smaller PAH molecules or fragments at higher combustion temperatures. The faster the flame reactions, the more complete the combustion and the faster the agglomeration processes, which in turn lead to higher fractions of larger PAH species. Third, the peak in the bimodal distribution of the PAH yield below 1.0 μm (Figure 4) may be due to condensation/deposition of PAHs, whereas the PAHs associated with the larger particles (i.e., the peak between 6 and 14 μm) may be partly due to surface chemical reactions between smaller PAH fragments in the gas phase and those adsorbed on the particle surface. Condensation will occur preferentially on smaller particles because of the larger amount of surface area, but chemical reaction may be driven by surface area or by the reactivity of the particle surface. A range of low and high molecular weight species will condense, but chemical reaction will tend to create higher molecular weight species. It is hypothesized that condensation dominates in the smaller particles and that chemical reaction dominates in the larger particles. This hypothesis is con-

sistent with the data presented in Table 2, which show that the PAHs associated with the larger particles are mostly of high molecular weight, while the ones on the smaller particles have a wide range of molecular weights. Further verification of the hypothesized surface or interfacial reaction of PAHs is needed before definitive conclusions can be reached.

The present experimental results also provide important insights into emission control strategies for PAHs from municipal solid waste incinerators. As shown in Figure 4, a relatively large amount of PAHs formed from polystyrene incineration are associated with the fine particles less than about 1.0 μm . The relatively large amount of PAHs associated with the smaller particles re-emphasizes the need for control of fine particulate emissions from incinerators.

Acknowledgments

Financial support for this study was provided by The Procter & Gamble Company. Special thanks are due to Tai-Gyu Lee (Aerosol and Air Quality Research Laboratory) for his assistance with the combustion experiments. We would also like to thank Staci Simonich (Procter & Gamble) for her help with the GC/MS chemical analysis methodology.

Literature Cited

- (1) Lin, W. Y.; and Biswas, P. *Combust. Sci. Technol.* **1994**, *101*, 29–43.
- (2) Durlak, S. K.; Biswas, P.; Shi, J. *J. Hazard. Mater.* **1997**, *56*, 1–20.
- (3) Tillman, D. A.; Rosii, A. J.; Vick, K. M. *Incineration of Municipal and Hazardous Waste*; Academic Press: San Diego, 1989.
- (4) Wheatley, L.; Leventis, Y. A.; Vouros, P. *Environ. Sci. Technol.* **1993**, *27*, 2885–2895.
- (5) Elomaa, M.; Saharinen, E. *J. Appl. Polym. Sci.* **1991**, *42*, 2819–2824.
- (6) World Health Organization. *J. Air Pollut. Control Assoc.* **1989**, *39*, 792.
- (7) Panagiotou, T.; Leventis, Y. *Combust. Flame* **1994**, *99*, 53–74.
- (8) Hawley-Fedder, R. A.; Parsons, M. L.; Karasek, F. W. *J. Chromatogr.* **1984**, *315*, 201–210.
- (9) Cullis, C. F.; Hirschler, M. M. *The Combustion of Organic Polymers*; Clarendon Press: Oxford, 1981.
- (10) Hepp, H.; Siegmann, K.; Sattler, K. *Chem. Phys. Lett.* **1995**, *233*, 16–22.
- (11) McKinnon, J. T.; Meyer, E.; Howard, J. B. *Combust. Flame* **1996**, *105*, 161–166.
- (12) Flagan, R. C.; Seinfeld, J. H. *Fundamentals of Air Pollution Engineering*; Prentice-Hall: Englewood Cliffs, NJ, 1988.
- (13) Biswas, P.; Li, X.; Pratsinis, S. E. *J. Appl. Phys.* **1989**, *65*, 2445–2450.
- (14) Biswas, P. In *Aerosol Measurement: Principles, Techniques and Applications*; Willeke, K., Baron, P., Eds.; Van Nostrand Reinhold: New York, 1992; pp 705–720.
- (15) Hart, K. M.; Pankow, J. F. *Environ. Sci. Technol.* **1994**, *28*, 655–661.
- (16) Turpin, B. J.; Liu, S. P.; Podolske, K. S.; Gomes, M. S. P.; Eisenreich, S. J.; McMurry, P. H. *Environ. Sci. Technol.* **1993**, *27*, 2441–2449.
- (17) Hewlett Packard. NIST/EPA/MSDC 54k Mass Spectral Database (NBS54k.I). 1990.
- (18) Rostad, C. E.; Pereira, W. E. *J. High-Resolut. Chromatogr. Chromatogr. Commun.* **1986**, *9*, 328–334.
- (19) Lee, M. L.; Vassilaros, D. L.; White, C. M.; Novotny, M. *Anal. Chem.* **1979**, *51*, 768–773.
- (20) Robertson, D. J.; Elwood, J. H.; Groth, R. H. *Chemical Composition of Exhaust Particles from Gas Turbine Engines*; 1979; EPA 68-02-2458.

Received for review October 15, 1997. Revised manuscript received April 14, 1998. Accepted April 22, 1998.

ES9709031